

Enzyme free direct detection of histamine in peanuts using novel γ - $\text{MnOOH-W}_3\text{O}_{10}$ nanostructures modified electrode

Amisha Kushwaha¹, Gajendar Singh¹, Umesh Kumar Gaur², Manu Sharma^{1*}

¹Central University of Gujarat, Gujarat

²Vitthalbhai Patel & Rajratna P. T. Patel Science College

*Corresponding author: Dr. Manu Sharma

Email address manu.sharma@cug.ac.in

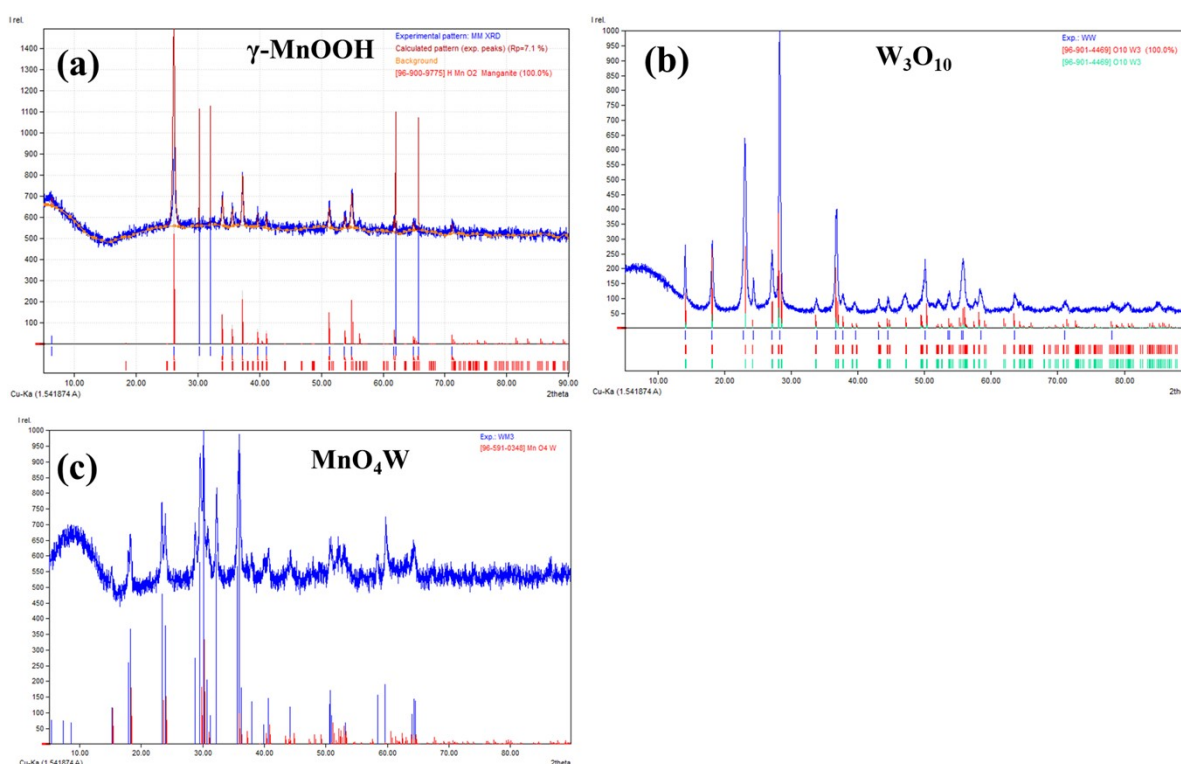


Fig. S1. Match 3 XRD analysis software computed results. (a) XRD spectra of γ -MnOOH with Match 3 XRD analysis software computed XRD pattern. (b) XRD spectra of W_3O_{10} with Match 3 XRD analysis software computed XRD pattern. (c) XRD spectra of MnO_4W with Match 3 XRD analysis software computed XRD pattern.

1.1 FTIR Analysis

There were nine characteristic peaks spotted at $\sim 450\text{ cm}^{-1}$, 491 cm^{-1} , 592 cm^{-1} , 657 cm^{-1} , 1081 cm^{-1} , 1149 cm^{-1} , 1619 cm^{-1} , 2075 cm^{-1} , and 2653 cm^{-1} wavenumbers. The peaks spotted at $\sim 450\text{ cm}^{-1}$, 491 cm^{-1} , and 657 cm^{-1} are related to the Mn-O bonding network. Peaks at 1081 cm^{-1}

and 1149 cm^{-1} are characteristic of hydroxyl vibrations in $\gamma\text{-MnOOH}$. While the peaks observed at $\sim 2653\text{ cm}^{-1}$ and 592 cm^{-1} are for the O-H stretching band associated with hydrogen band of O-H...O of $\gamma\text{-MnOOH}$. Peak spotted at 1619 cm^{-1} could be due to the bending modes of water molecules adsorbed at the surface of $\gamma\text{-MnOOH}$. The FT-IR of MNO sample was in good agreement with M.S. Selim et al. recent report[30]. In case of WO sample, the FT-IR bands spotted at $\sim 451\text{ cm}^{-1}$, and 649 cm^{-1} are related to the W-O bonding network. The peak spotted at $\sim 991\text{ cm}^{-1}$ could be related to the W=O bonding network. The peak located at $\sim 1605\text{ cm}^{-1}$ could be due to the bending modes of water molecules adsorbed at the surface of W_3O_{10} . The broad peak ranging from $3500\text{-}3600\text{ cm}^{-1}$ could be due to the O-H stretching vibrations. The FT-IR of WO sample was found well matched with Shouli Bai et al. research work[31]. FTIR of MW is showing the broad band at 3437 cm^{-1} in the vibration of O-H bond of the surface hydration. The band at 1637 cm^{-1} corresponds to the H-O-H deformation vibration of surface hydroxyl group. The peak spotted at 872 cm^{-1} and 829 cm^{-1} indicate the asymmetric and symmetric stretching vibration mode of W-O bond at the WO_2 terminal group of MnWO_4 . Strong band at 706 cm^{-1} is related to the asymmetrical stretching vibrations for W-O bond in $(\text{W}_2\text{O}_4)_n$ chain, 621 cm^{-1} indicate the presence of stretching vibration of Mn-O bond. The Mn-O-Mn bonding network related to the stretching vibration bond can be seen at 516 cm^{-1} [32].

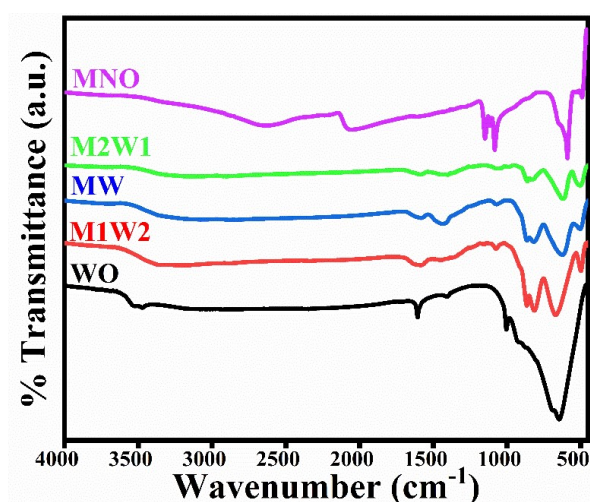


Fig. S2 FT-IR spectra of MM, M2W1, MW, M1W2

1.2 UV-Vis Analysis

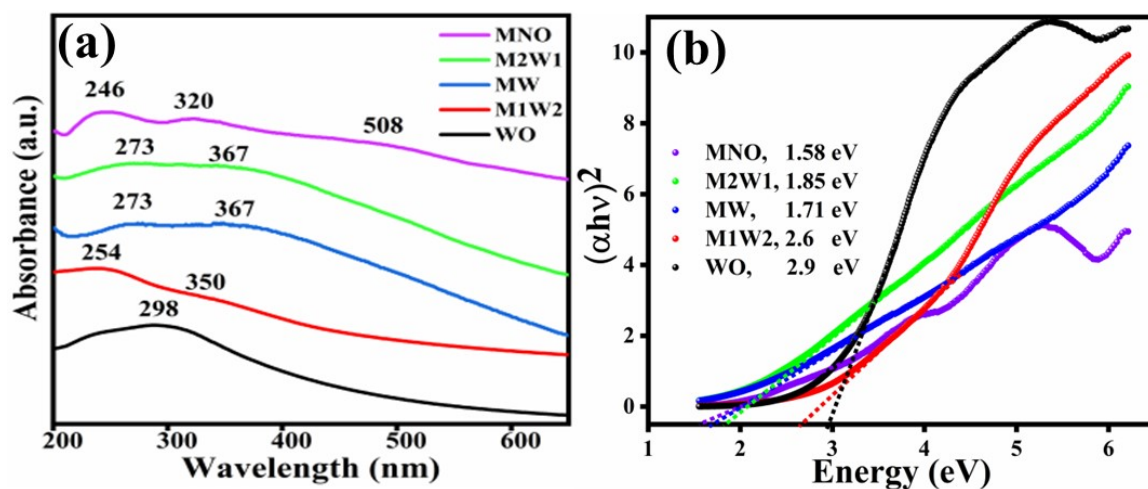


Fig.S3 (a) UV-Vis. spectra of MM, M2W1, MW, M1W2 and (b) Tauc's plot for bandgap analysis of MM, M2W1, MW, M1W2.

1.3 Band positions and impedance analysis of MNO@GCE, WO@GCE, and MW@GCE

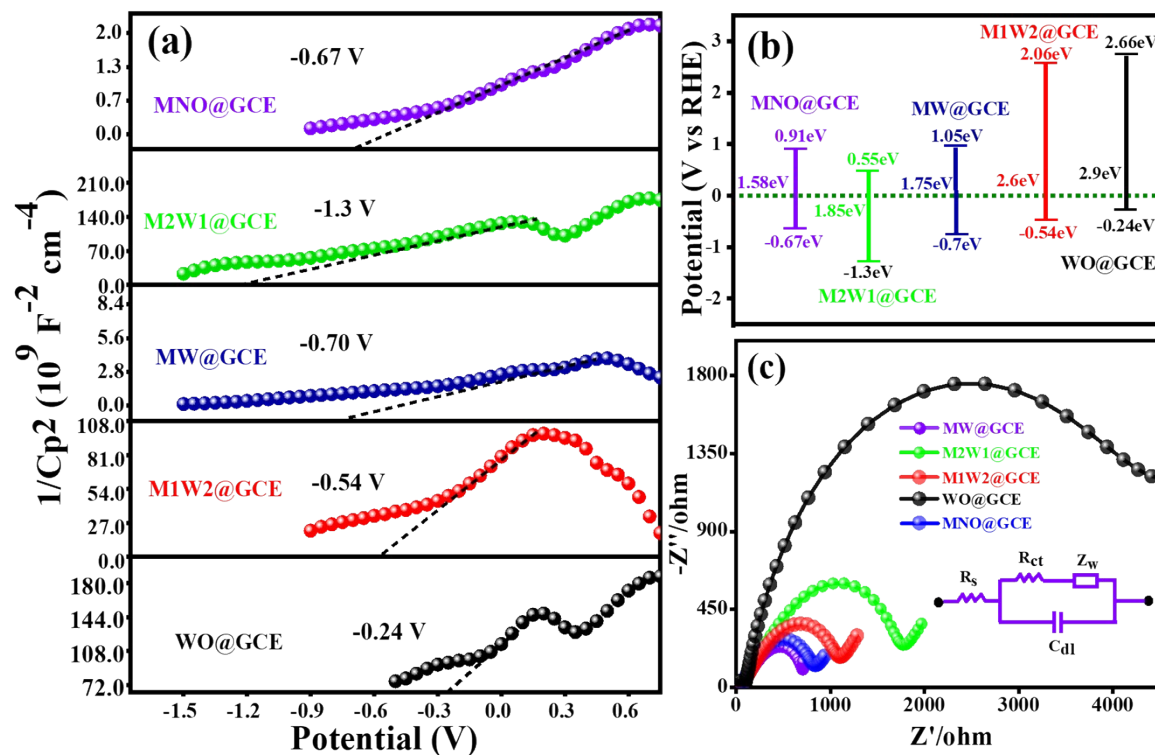


Fig. S4 (a) Mott-Schottky analysis of MNO@GCE, WO@GCE, M1W2@GCE, MW@GCE, and M2W1@GCE (b) Estimated band structure diagram for MNO@GCE, WO@GCE, M1W2@GCE, MW@GCE, and M2W1@GCE (c) Nyquist plots for MNO@GCE, WO@GCE, M1W2@GCE, MW@GCE, and M2W1@GCE.

The identification of flat band potentials of MNO@GCE, WO@GCE, MW@GCE, M1W2@GCE and M2W1@GCE electrodes was carried out using Impedance-Potential (IMPE) technique between -1.5 V – 0.7 V potential window with 1000 Hz frequency. The conduction band position for MNO@GCE, WO@GCE, MW@GCE, M1W2@GCE and M2W1@GCE electrodes was found to be -0.67 V, -0.24 V, -0.70 V, -0.54 V, and -1.30 V respectively as shown in **Fig. S4a**. **Fig. S4b** represents the estimated band structure diagram for MNO, WO, MW, M1W2 and M2W1 suggesting the applicability of as prepared nanomaterials for various electrochemical applications rather than electrochemical sensing. For impedance analysis, EIS technique was performed to illustrate the facile electron transfer behavior during the experiment. At 5 mV signal amplitude and 0.1 Hz-100 Hz frequency range, comparative Nyquist plots of MNO@GCE, WO@GCE, M1W2@GCE, MW@GCE, and M2W1@GCE are shown in **Fig. S4c**. Its employees that MW@GCE electrode possesses smallest hemisphere suggesting the good electron transport rate between electrode surface and electrolyte. Constructed equivalent circuit of this Nyquist plot was having resistance of solution (R_s) and charge transfer (R_{ct}); double layer capacitance (C_{dl}); and Warburg impedance (Z_w) shown in the inset of **Fig. S4c**. Therefore, the R_s and R_{ct} was calculated are 76.14 Ω and 628.21 Ω respectively.

1.4 Effect of NaOH electrolyte concentration, MW loading and scan rate on HS oxidation

For electrochemical detection of biomolecules electrolyte plays the significant role. Recently, Jaroslava Svarc-Gajic et al. research group examined the role of supporting electrolyte for the HS oxidation. They found the superior suitability of NaOH as electrolyte over NH_4OH , Na_2CO_3 , and KOH electrolytes for HS oxidation. Further, they also checked the influence of different concentration $0.1\text{--}1.5\text{ mol L}^{-1}$ of NaOH. 0.5 mol L^{-1} concentration of NaOH was suitable for Chronopotentiometry oxidation of HS [25]. In a similar study, Prangthip Nakthong et al. have also checked the influence of electrolyte over HS oxidation. They performed square wave voltammetry for HS oxidation in PBS buffer ($3.0\text{--}9.0\text{ pH}$) but the enhanced signal was observed in 0.2 M NaOH electrolyte[35].

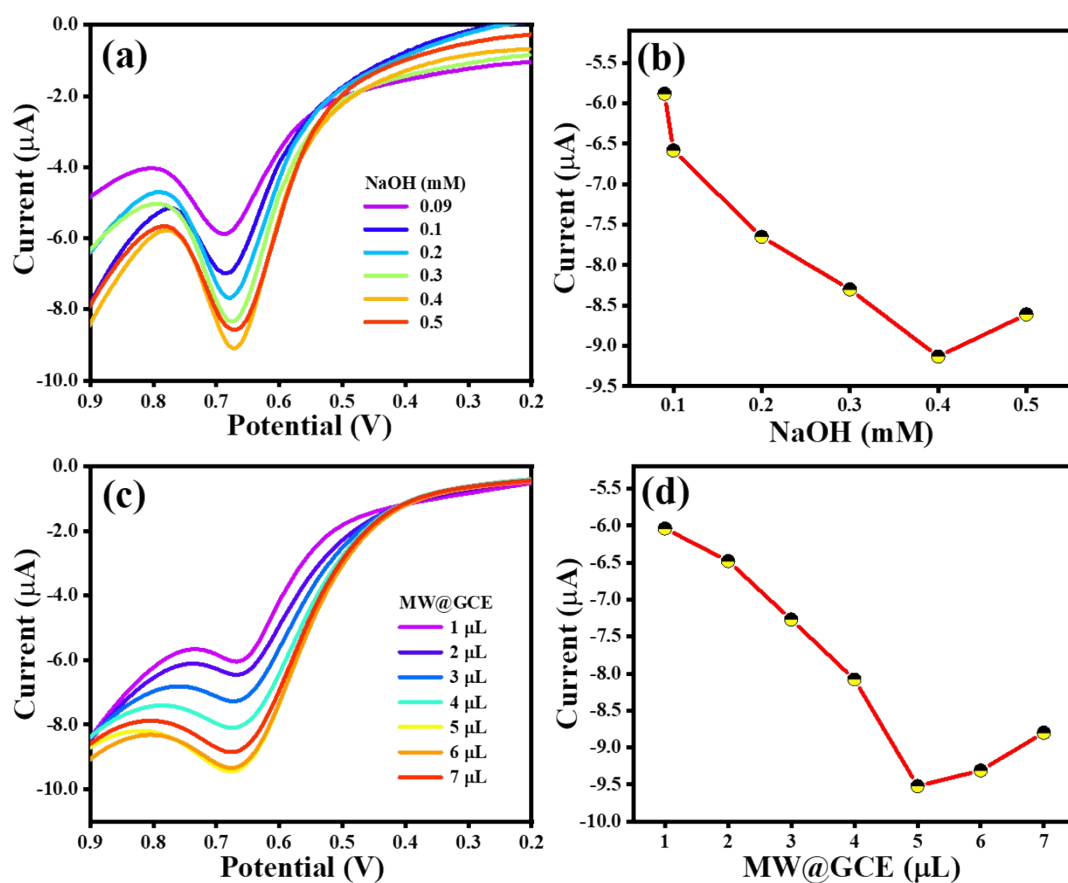


Fig.S5. (a) Effect of NaOH concentration over HS oxidation. (b) Dependence of HS oxidation current over NaOH concentration. (c) Effect of MW loading on GCE over HS oxidation. (d) Dependence of HS oxidation current over MW loading on GCE.

Therefore, we have used NaOH electrolyte for voltametric detection of HS. However, the influence of NaOH electrolyte concentration has been identified for HS oxidation. **Fig. S5a** indicates the DPV responses in NaOH electrolyte (0.09 – 0.5 mM) containing 0.25 μ M HS. The highest signal of HS oxidation at 0.66 V was observed for 0.4 mM NaOH electrolyte concentration. HS oxidation current over NaOH electrolyte different concentration is shown in **Fig. S5b**. The fact behind the Electrochemical oxidation could be due to the strong base NaOH molecule interferes with two groups of HS N- in aliphatic amino group having pK_a value of \sim 9.4 and imidazole ring with $pK_a = \sim$ 5.8. We believe that the HS imidazole ring gets deprotonated in alkaline medium to negative charged form which further simply electrochemically oxidized. As shown in **Fig. S5b**, the oxidation current for HS increases with the NaOH concentrations from 0.09 – 0.4 mM but at 0.5 mM it drastically decreased suggesting 0.4 mM NaOH concentration is optimal for further study. Like electrolyte pH, and electrolyte concentration, the amount of catalyst plays a key role in electrochemical detection of biomolecules. Therefore, we investigated the effect of MW loading on GCE for the better performance towards HS oxidation. **Fig. S5c** indicates the DPV response of 0.25 μ M HS containing electrolyte using GCE fabricated by 1-7 μ L of 0.5mg/mL MW loading. **Fig. S5d** depicts the dependence of HS oxidation current over different amount of MW loaded GCE. The HS oxidation current increases with 1-5 μ L of MW but further it decreases for 6-7 μ L. The less oxidation of HS for higher amount of MW could be due to the thickness of MW at GCE surface which resist the smooth transportation of electrons between electrode and HS containing electrolyte.

